profile. While non-CAD-sEVs did not statistically differ from PBS nor untouched groups, CAD-sEVs increased the mRNA level of IL1a, IL1b, TNFa and decreased MRC1. Proteomics revealed that PF-sEVs from CAD patients carried higher amounts of pro-inflammatory molecules (ICAM-1 and IL18) compared to NonCAD control. Bioinformatics analysis showed that 861 miRNAs were decreased in the PF-sEVs from CAD patients compared to non-CAD. miRNA targets prediction and pathway analyses reported that clusters of deregulated miRNAs could regulate CD36 and SRB1 which were shown to be decreased in CAD-sEVs treated macrophages. Human PF-cells revealed a reduced expression of CD36 on PF-macrophages.
Conclusions We demonstrate, for the first time, that sEVs isolated from the PF of CAD patients induce a proinflammatory profile of human macrophages and that target crucial lipid metabolism pathways. These clinically relevant results could drive to decipher improved therapeutics able modulate the epicardial/myocardial immune response in CAD patients.

BS26 ROLE OF KMT2C, A HISTONE METHYLTRANSFERASE IN THE DEVELOPMENT OF COMPACTED MYOCARDIUM

Sabu Abraham. *University of Manchester, Core Technology Facility, 46 Grafton Street, Manchester, GTM M13 9NT UK*

10.1136/heartjnl-2022-BCS.206

Epigenetic gene regulation has been increasingly established as a pivotal molecular mechanism driving heart development and its aberrant regulation has been implicated in congenital heart diseases. KMT2C is a histone methyltransferase enzyme that mediates the Histone 3 lysine 4 (H3K4) methylation that denotes active promoters and enhancers. Our previous work identified a number of de novo variants in KMT2C gene in nonsyndromic Tetralogy of Fallot patients. Global deletion of delta SET domain region of Kmt2c gene that harbour methyltransferase enzymatic activity resulted in neonatal lethality in mice. Histological analysis of knockout mice embryonic heart revealed ventricular septal defect (with and without an overriding aorta) with a low penetrance but also displayed a consistent phenotype resembling ventricular non-compaction. Embryonic hearts from the knockout mice at the e16.5 stage of development displayed a significantly thinner ($p<0.05$) compact myocardium of the left ventricle compared to the wild-type littermates. In order to get insights into the molecular mechanism for this phenotype, we carried out RNA sequencing experiments in ventricles of e16.5 embryonic hearts from mice with a homozygous deletion and wild type littermates. A significant decrease in gene expression is observed in many of the extracellular matrix (ECM) genes, especially elastin ($p<1.0E-6$), various subtypes of collagens, fibronectin, and integrins. We also found an altered expression of genes important for ECM homeostasis, e.g. MMPs, and ventricular trabeculation/compaction, e.g. Notch1. ECM is known to play important role in heart development, including trabeculation and formation of compacted myocardium. Our data suggest an important role played by Kmt2c in regulating ECM homeostasis and the formation of compacted myocardium.

BS27 ECHOCARDIOGRAPHIC EVALUATION OF LEFT VENTRICULAR FUNCTION AND MYOCARDIAL DEFORMATION IN A REPERFUSED MOUSE MODEL OF MYOCARDIAL INFARCTION

Zhiping Feng. *UCL, Paul O'Gorman Building, 72 Huntley Stree, Finchley, London, LND WC1E 6DD UK*

10.1136/heartjnl-2022-BCS.207

We evaluated the feasibility and accuracy of four-dimensional preclinical ultrasound (4D-US) and speckle-tracking imaging (STI) for monitoring changes in function post reperfused myocardial infarction (MI).
Methods Seventeen female mice (age = 10–12 wk) underwent ligation of the left anterior descending coronary artery. Cardiac MRI (Varian 9.4T) and echocardiographic images (Visualsonics 3100) were acquired at 2weeks (n=6) or8weeks (n=11) post-surgery. Ejection fraction was calculated and then compared between 4D-US, MRI, M-mode and Simpson's multi slice at each time point. Eight healthy mice and seventeen MI mice were used for STI strain analysis.
Results All ultrasound methods calculated ejection fractions that correlated with MRI. However, 4D-US provided the strongest agreement, outperforming M-mode and Simpson's multi slice (4D-US: $R2= 0.81$, M-mode: $R2= 0.55$, Simpson's: $R2= 0.73$) (table 1). STI-derived measures of global strain were significantly lower in the MI group in all dimensions ($P < 0.005$). (Figure 1 A) For regional strain analysis, circumferential strain values in MI were significantly lower in antero-lateral and septal regions compared with control mice ($P < 0.001$). (Figure 1 B). The longitudinal strain and radial

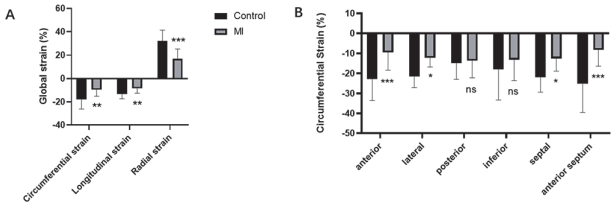

Abstract BS27 Figure 1 A, Differences in global strain between MI and control groups. B, Differences in regional strain in circumferential between MI and control groups. ns: not statistically significant; *P < 0.05 **P < 0.005, ***P < 0.001.

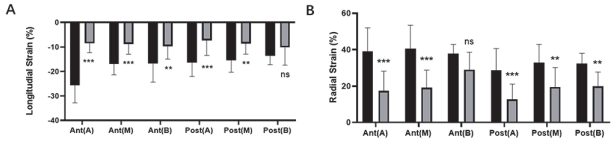

Abstract BS27 Figure 2 A-B, Differences in regional strain in longitudinal and radial between MI and control. Ant(A), anterior apical; Ant(M), anterior mid; Ant(B), anterior basal; Post(A), posterior apical; Post(M), posterior mid; Post(B), posterior basal. ns: not statistically significant; **P < 0.005; ***P < 0.0001.